Article

UDC 621.785.6

https://doi.org/10.31489/2025PH4/61-73

Received: 20.08.2025
Accepted: 01.09.2025

D.B. Buitkenov[1], N.S. Raisov[1]✉, N.Ye. Bazarov[2],
G.T. Tleubergenova[1], A.K. Khassenov[3], D.Zh. Karabekova[3]

*[1]Research Center "Surface Engineering and Tribology",
Sarsen Amanzholov East Kazakhstan University, Ust-Kamenogorsk, Kazakhstan;
[2]LLP "PlasmaScience", Ust-Kamenogorsk, Kazakhstan;
[3]Buketov Karaganda National Research University, Karaganda, Kazakhstan*

Tribological Performance of Self-Fluxing Ni-Based Coatings Deposited by Gas-Flame Spraying

In the present study, a comprehensive analysis of the microstructure, phase composition, surface morphology, and tribological properties of self-fluxing NiCrFeBSiC alloy coatings produced by flame spraying was conducted. Particular attention was paid to evaluating the influence of different heat treatment regimes — flame heating and furnace heating — on the coating characteristics. X-ray diffraction analysis revealed the formation of the $FeNi_3$ phase, along with Cr_7C_3, $Cr_{23}C_6$ carbides and boride compounds, which significantly affect wear resistance. Goniometric measurements showed that the highest surface hydrophobicity (contact angle of 89.6°) was achieved after furnace heat treatment. Scanning electron microscopy and profilometry studies established that furnace heating provides the densest and smoothest structure with the lowest surface roughness (Ra = 13.388 μm). Tribological tests confirmed that this treatment provides the lowest and most stable coefficient of friction (0.138 ± 0.003), which correlates with the microstructural features of the wear track. The obtained results demonstrate the high efficiency of furnace heat treatment in enhancing the performance characteristics of NiCrFeBSiC-based coatings.

Keywords: self-fluxing alloys, gas-flame spraying, NiCrFeBSiC, heat treatment, steel 45

✉*Corresponding author*: Raisov, Nurmahanbet, nurmakhanbetraisov@gmail.com

Introduction

Structural materials with high performance characteristics capable of operating under severe conditions—such as increased friction, exposure to aggressive environments, and thermal loads—are in great demand. Such service conditions inevitably lead to wear of components, resulting in frequent repairs, replacement of parts, and an increase in production costs, which in turn causes significant economic losses [1, 3].

However, manufacturing components entirely from expensive wear-resistant materials is associated with a sharp rise in production costs and technological difficulties during machining. A rational solution to this problem is the application of wear-resistant coatings or the restoration of worn elements, which makes it possible to significantly extend their service life [1]. Among such solutions, a special place is occupied by coatings made of self-fluxing nickel-based alloys, which have found wide application in mechanical engineering [2, 3]. Thermal spray coatings, including plasma-sprayed ones, based on Ni-Cr-Fe-B-Si-C systems are used to increase the wear resistance of working surfaces of components. NiCrFeBSiC alloys have proven

themselves in service under conditions of intensive friction—in coal boiler components, heat exchangers, turbines, tools, extruders, plungers, rolling mill rolls, and agricultural machinery. These coatings are characterized by high resistance to adhesive wear and corrosion both at ambient and elevated temperatures. To improve their performance properties, the coatings are subjected to remelting after deposition. Due to the presence of boride and carbide phases in their structure, such materials exhibit enhanced wear resistance under abrasive conditions [4, 7].

The formation of the required tribotechnical properties of remelted Ni-Cr-Fe-B-Si coatings is possible only under strictly defined heat treatment regimes (in the range of 1000–1373 K), since these alloys belong to eutectic systems and are highly sensitive to thermal process parameters [5, 6]. Remelting can be carried out by various methods: flame heating, furnace heating, or laser treatment. Although a number of studies [6–10] have examined in detail the structure, properties, and phase transformations during the remelting of self-fluxing NiCrBSiC coatings, issues related to their tribological behavior and wear mechanisms under friction conditions have not been sufficiently addressed. In this regard, the present work is devoted to the investigation of the tribological behavior of NiCrFeBSiC coatings produced by flame spraying followed by remelting.

Materials and methods

As the substrate material, structural carbon steel grade AISI 1045 was selected. This steel is widely used in industry for the production of shaft gears, crankshafts, camshafts, gears, spindles, tires, cylinders, cams, and other normalized, tempered (improved), and surface-hardened components that require increased strength. According to ASTM A331, AISI 1045 steel has the following composition (Table 1).

Table 1

Chemical composition of steel 1045

C	Si	Mn	Ni	S	P	Cr	Cu	Fe
0.42–0.5	0.17–0.37	0.5–0.8	< 0.3	< 0.04	< 0.035	< 0.25	< 0.3	base

A steel rod of carbon steel grade AISI 1045 with a diameter of 50 mm was cut into disks 5 mm thick. The surface was mechanically treated by grinding with abrasive paper up to P600 grit. To improve the adhesion of the applied coating, the disk surfaces were additionally treated by abrasive blasting using electrocorundum (Al_2O_3) with a particle size of 40 μm. After sandblasting, residual abrasive particles and dust were removed by blowing with compressed air. In order to eliminate organic and inorganic contaminants (oils, oxide films), the samples were cleaned in an ultrasonic bath using technical-grade ethanol. The ultrasonic cleaning was carried out for 10 minutes at a frequency of 40 kHz and a solution temperature not exceeding 35 °C. Prior to coating deposition, the samples were preheated to 200–250 °C by flame heating to improve adhesion to the substrate. The surface temperature was monitored using a RoHS-compliant infrared pyrometer, model DT8016E, with a measurement range of –50 °C to 1600 °C and an accuracy of ±2 °C.

The powders have a spherical structure with particle sizes ranging from 100 to 200 μm (Fig. 1).

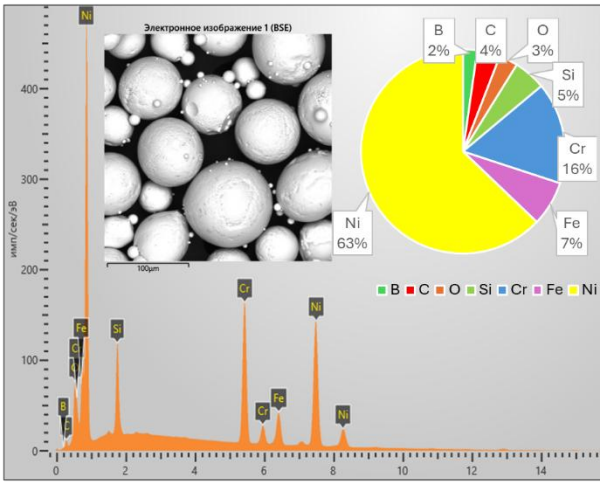

Figure 1. Morphology of self-fluxing NiCrFeBSiC powder

For the coating deposition, a flame spraying unit manufactured by Metal Coat was used, equipped with a 6PM-II powder gun and an MPF700 powder feeder. The general view of the setup and the schematic diagram of the spray gun are shown in Figure 2. The operating principle of this unit consists in melting powder particles by combustion of a gas mixture composed of acetylene and oxygen. Compressed air was used both for powder transport and for cooling the barrel. The air supplied from the compressor passed through a filter integrated into the outlet pressure regulator in order to prevent contamination of the powders with motor oil particles.

The supply of the gas mixture was monitored and controlled by gas flow meters and a compressed-air control unit. In addition, the system included a powder feed adjustment function to reduce material consumption. The particle flow velocity and flame temperature were measured using a high-speed Tecnar Accuraspray 4.0 diagnostic system (11-12).

The spraying parameters were selected in such a way that the porosity of the coatings did not exceed 10 % (ISO/TR 26946:2011). The spraying regime is presented in Table 2.

Table 2

Gas flame spraying parameters for obtaining coatings

Operation gas	Oxygen	25 NLPM
	Acetylene	15 NLPM
Powder carrier gas	Air	37 NLPM
Spraying distance	200 mm	
Spray time	30 s	

The substrate of AISI 1045 steel was preheated by the flame method to a temperature corresponding to low-temperature tempering, 200–250 °C. After preheating, the microhardness of AISI 1045 steel was measured using the Vickers method at 15 different surface points. Before heating, the average microhardness value of AISI 1045 steel was 196.7 ± 5.3 $HV_{0.3}$, while after heating it increased to 298.6 ± 5.7 $HV_{0.3}$.

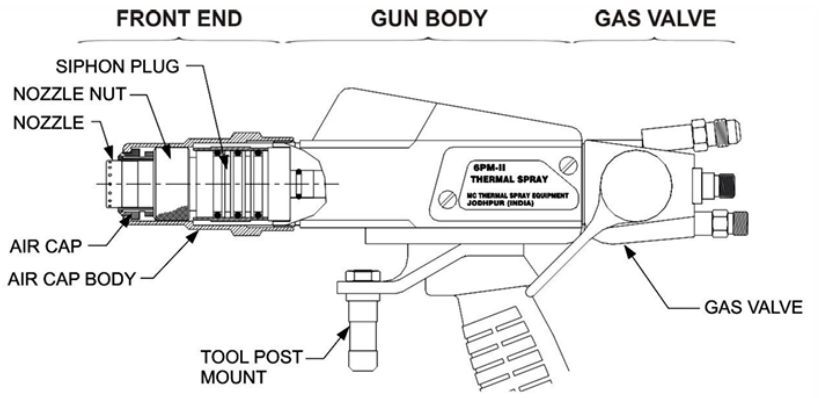

Figure 2. Flame spray gun diagram

The heat treatment of the coatings was carried out by two methods at 1025 °C for 5 minutes: (1) flame heating and (2) furnace heating.

The coating morphology was studied using a SEM 3200 scanning electron microscope (China), equipped with an electron probe attachment for local microanalysis: a Bruker energy-dispersive spectrometer (EDS).

X-ray diffraction (XRD) analysis of the initial powder and coatings was performed on a PANalytical X'PERT PRO diffractometer using CuKα radiation. The diffraction data were collected in the 2θ range of 10–90° with a step size of 0.02° and a counting time of 0.5 s per step.

Tribological tests of the coatings were conducted using a ball-on-disk configuration. As a counter body, a 100Cr6 steel ball with a diameter of 6 mm was used. The applied load was 10 N, sliding speed 5 cm/s, track radius 2 mm, and sliding distance 200 m.

Potentiodynamic polarization curves were recorded on a CorrTest CS310 potentiostat using a three-electrode cell, as shown in Figure 3. The scanning rate was 0.5 mV/s within a potential range of –0.8 V to

+0.8 V. A 3.5 % HCl solution was used as the electrolyte. A platinum mesh served as the working electrode, while saturated silver chloride electrodes were used as both reference and auxiliary electrodes. The current and potential data obtained were processed with the CorrTest CS310 software, which was used to construct polarization curves providing information on corrosion potential, corrosion current, and passivation behavior [9].

Adhesion strength tests were performed in accordance with ASTM C633-15 on a WDW-100kN tensile testing machine, equipped with a self-aligning load application module. For the adhesion test, samples with a diameter of 25.4 mm and a thickness of 7 mm were prepared. Prior to spraying, the samples were subjected to sandblasting and cleaned in an ultrasonic bath with ethanol. The tensile loading rate was 0.020 mm/s [13–17].

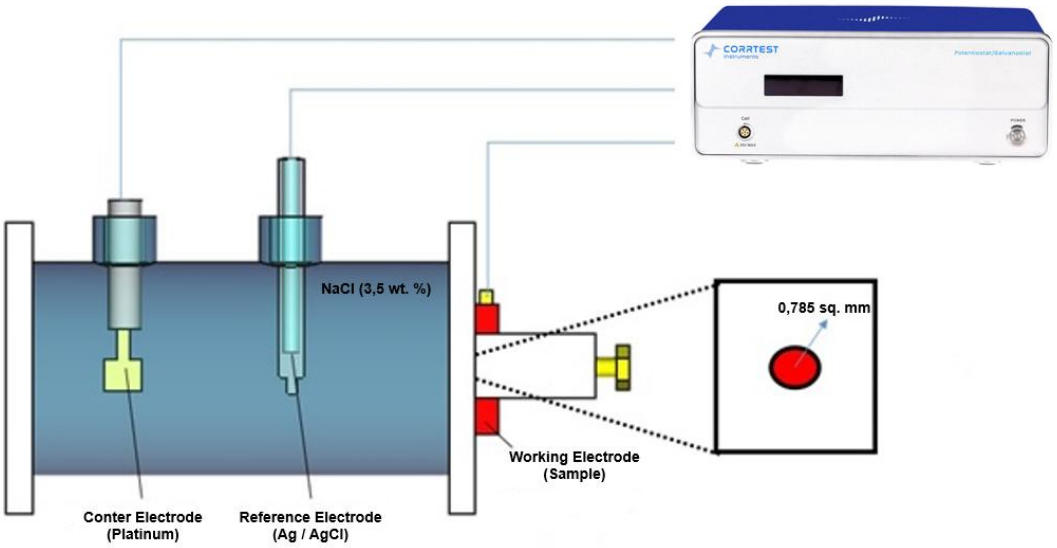

Figure 3. Schematic diagram of the setup Potentiostat CS310
for conducting an electrochemical corrosion experiment [9]

Results and discussion

To study the microstructure and elemental composition of the coating based on NiCrFeBSiC, energy-dispersive X-ray spectral analysis (EDS) was carried out as part of scanning electron microscopy (SEM). The results are presented in Figure 4 in the form of element distribution maps and a summary table of mass fractions.

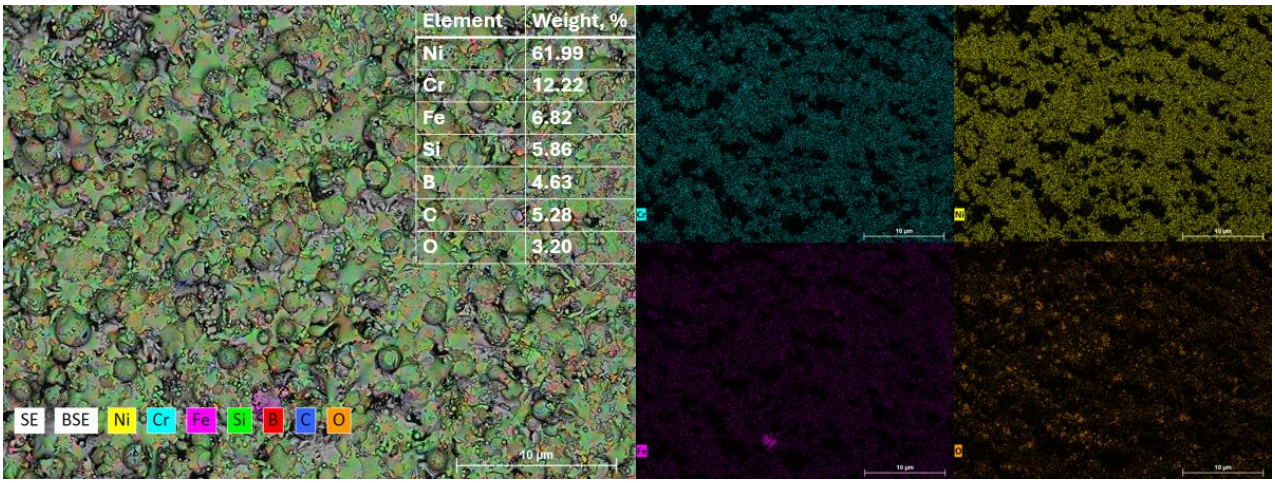

Figure 4. Map of distribution of elements on the surface of coatings made of self-fluxing NiCrFeBSiC powder

According to EDS analysis, the coating consists of the following elements (wt.%): Ni — 61.99 %, Cr — 12.22 %, Fe — 6.82 %, Si — 5.86 %, B — 4.63 %, C — 5.28 %, and O — 3.20 %. The combined

SEM–EDS mapping shows a uniform distribution of nickel (yellow), chromium (blue), iron (purple), silicon (green), boron (red), and carbon (orange).

Figure 5 presents the XRD patterns of the initial powder and coatings, designated as SF1, SF2, and SF3, which differ in the type of thermal treatment. Coating SF1 corresponds to the as-sprayed layer without additional heat treatment, SF2 represents the coating subjected to flame heating, and SF3 is the coating after furnace annealing.

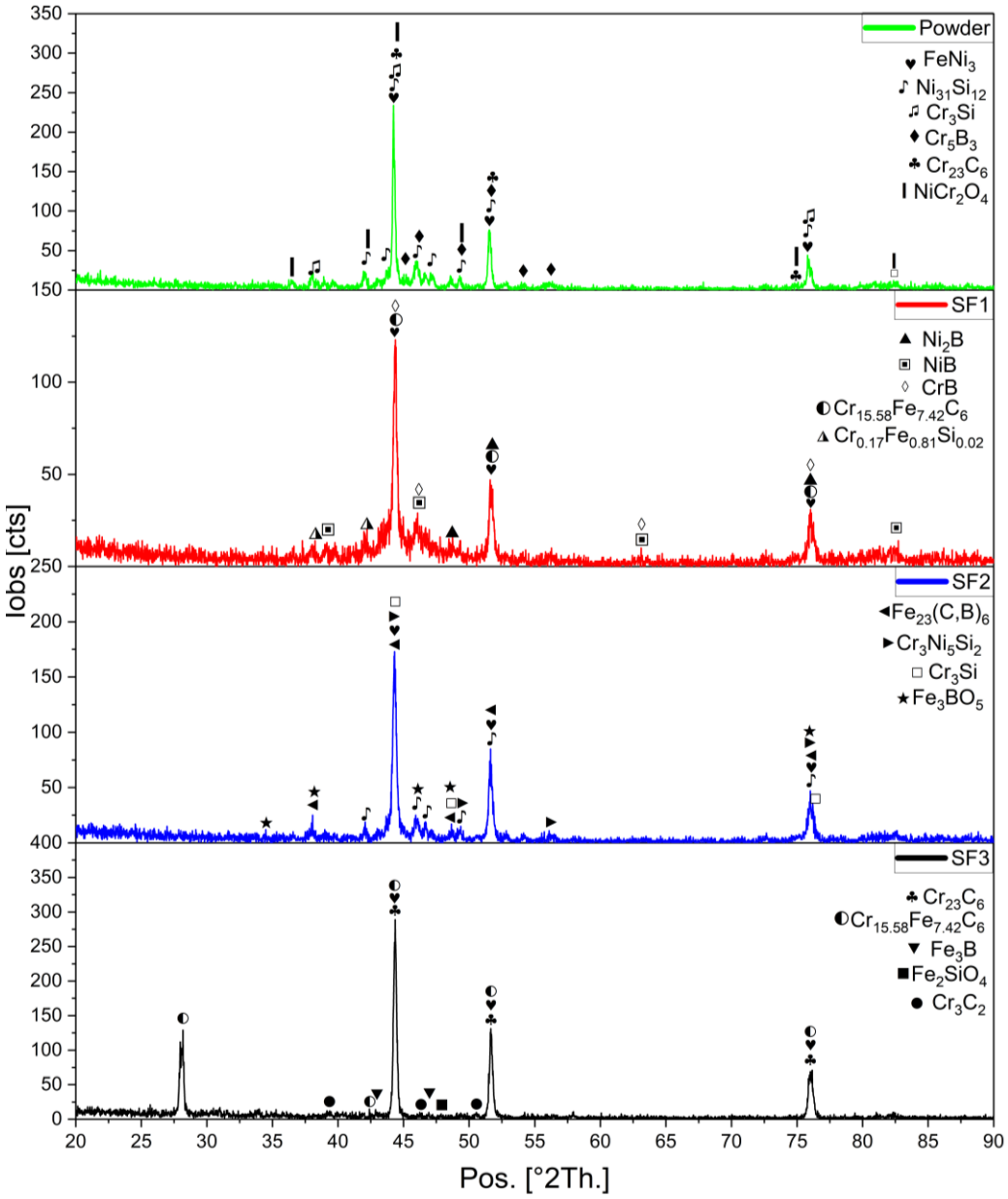

Figure 5. XRD spectra of powder and NiCrFeBSiC coatings: (SF1) without heat treatment, (SF2) after heating with a flame of a gas flame gun, (SF3) after heating in a furnace

Analysis of the diffraction patterns of the initial powder revealed the presence of $FeNi_3$, $Ni_{31}Si_{12}$, Cr_3Si, Cr_5B_3, $Cr_{23}C_6$, and $NiCr_2O_4$ phases, which is typical for nickel-based composite powders with boride–silicide and oxide inclusions. After flame spraying and subsequent heat treatment, significant changes in the phase composition of the coatings were observed [18-19].

In coating SF1, the phases Ni_2B, NiB, CrB, as well as carbide structures of the $Cr_{15.58}Fe_{7.42}C_6$ type and silicide $Cr_{0.17}Fe_{0.81}Si_{0.02}$ were identified, indicating the formation of new compounds during spraying while retaining part of the boride components of the initial powder. Coating SF2, subjected to flame heating, exhib-

ited a more complex phase composition: $Fe_{23}(C, B)_6$, $Cr_3Ni_5Si_2$, Fe_3BO_5, along with residual $FeNi_3$ and Cr_3Si. This suggests active interfacial reactions and diffusion processes enhanced by localized heating.

The SF3 coating, which underwent furnace heat treatment, contained phases such as $Cr_{23}C_6$, $Cr_{15.58}Fe_{7.42}C_6$, Cr_3C_2, Fe_3B, and Fe_2SiO_4 [20–23]. The predominance of stable carbides and borides combined with the minimal content of oxide phases indicates that furnace annealing promotes the formation of thermodynamically stable equilibrium structures, ensuring a dense and ordered microstructure of the coating.

Thus, the post-spraying thermal treatment regime has a decisive influence on the phase composition of the coatings. Flame heating promotes the formation of complex boride–silicide phases, whereas furnace annealing favors the stabilization of carbide structures and the reduction of oxide content, which may positively affect the performance properties of the coatings.

Such phase behavior is consistent with literature data, which note that heat treatment promotes the formation of stable strengthening phases in Ni-based coatings [24–26].

Figure 8 clearly shows that subsequent heat treatment significantly reduces the coating thickness, as well as the number and size of pores. This trend occurs due to more effective particle melting and the filling of pores with molten material [8]. The highest porosity was recorded in sample SF1, which did not undergo any additional heat treatment. The high porosity value indicates the presence of a large number of unmelted particles.

In coating SF2, which was subjected to short-term flame heating, porosity decreased almost 2.5 times compared to the untreated coating. This indicates partial densification of the near-surface layers and the occurrence of self-fluxing under the influence of temperature (Fig. 6*b*). The lowest porosity was observed in sample SF3, which underwent furnace heating. The furnace provides more uniform and prolonged heating, which promotes active self-fluxing and improved bonding between coating particles. As a result, the structure becomes denser and more homogeneous (Fig. 6*c*) [24].

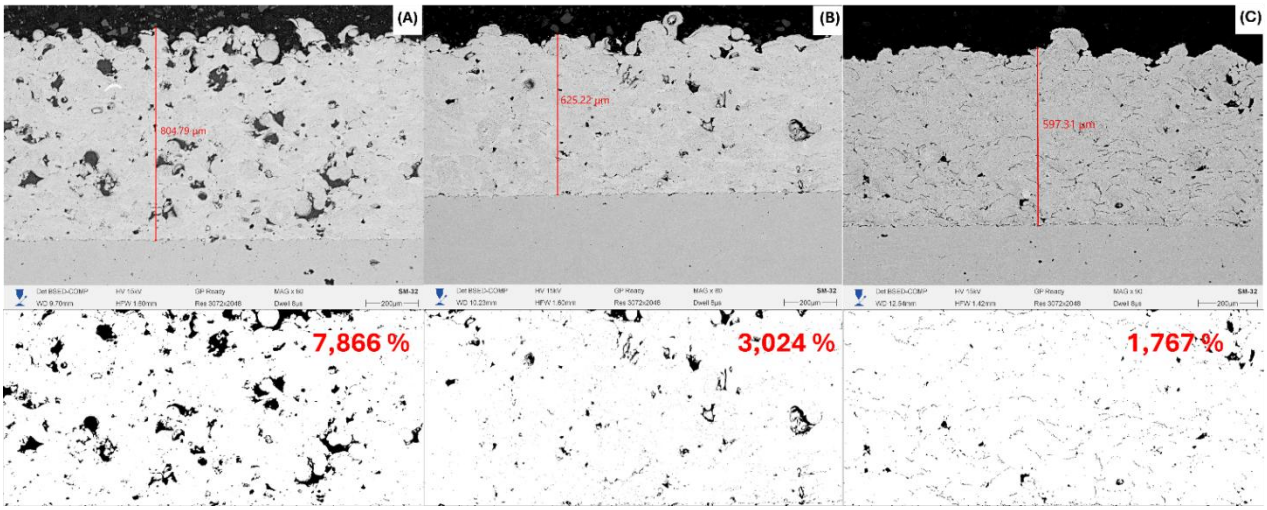

Figure 6. Study of the porosity and thickness of NiCrFeBSiC coatings on a cross section:
(*a*) without heating — SF1, (*b*) flame heating — SF2, (*c*) furnace heating — SF3

For a comprehensive evaluation of the morphology and surface topography of NiCrFeBSi-based coatings subjected to different heat treatment regimes, studies were carried out using SEM and profilometry. Figure 7 shows surface micrographs (top row) and the corresponding surface roughness profiles (bottom row), reflecting the actual height deviations in the selected areas. The SEM images demonstrate the typical microstructure of a thermally sprayed coating, characterized by a dense yet moderately porous structure, which results from the partial melting of particles during spraying [25]. Good interparticle bonding indicates that sufficient temperature was achieved during deposition. A decrease in the Ra parameter from 31.860 µm (as-sprayed) to 13.388 µm (furnace-treated) demonstrates a clear trend towards improved surface quality with the application of heat treatment. The SEM micrographs confirm that thermal treatment promotes densification of the structure, a reduction in porosity, and surface smoothing. The obtained results indicate a significant influence of heat treatment on the morphological and tribological properties of the coatings and highlight the advantages of uniform furnace heating compared to flame heating [26].

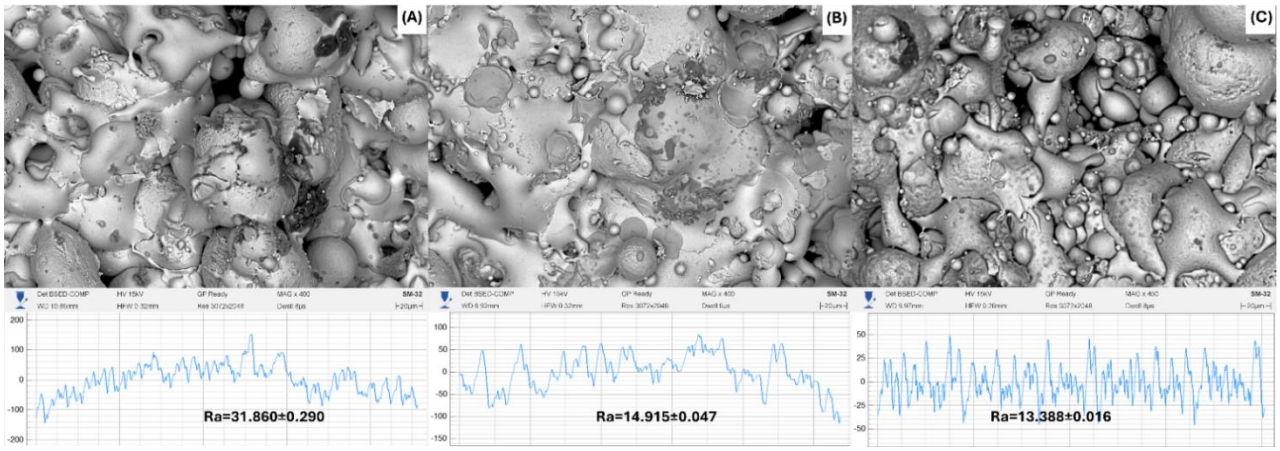

Figure 7. Micrographs of surfaces (top row) and corresponding roughness profile graphs (bottom row): (*A*) without heat treatment SF1, (*B*) after gas flame heating SF2, (*C*) after heating in a furnace SF3

Tribological tests were conducted to test the wear resistance of the coatings. The results are shown in Figure 8. According to the results of tribological tests with dry friction, it was found that subsequent heat treatment reduces the friction coefficient, thus thermal gas-flame heating and furnace treatment reduced the friction coefficient by 6 times on average for both types of treatment.

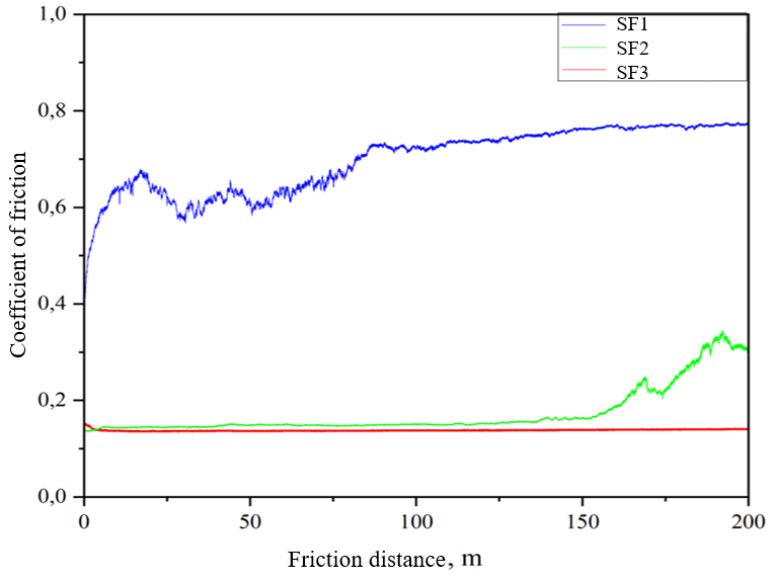

Figure 8. Results of tribological tests of coatings using the “ball-on-disk” scheme under dry friction: (SF1) without heat treatment, (SF2) after gas-flame heating, (SF3) after heating in a furnace

The most stable and lowest coefficient of friction, $\mu = 0.138 \pm 0.003$, was observed for coating SF3, which underwent furnace heat treatment at 1025 °C followed by slow cooling. The friction coefficient remained nearly constant along the entire wear track, indicating structural uniformity and high quality of the hardened surface, which suggests a reduction in microfractures [27–28]. In the case of flame heating (1025 °C, acetylene–oxygen flame), the coefficient of friction was $\mu = 0.173 \pm 0.050$. Moreover, beginning at a sliding distance of 150 m, an increase in the coefficient of friction was recorded, pointing to a change in the wear mechanism. This trend may be associated with localized densification of the coating structure during flame heating. Although no abrupt fluctuations of the friction coefficient were observed, significant local morphological changes may occur that are not fully reflected in the integral tribometric curve. As shown in [11], under localized temperature spikes and contact with hard inclusions (borides, carbides), plastic deformation of the softer binder matrix can occur, accompanied by strain hardening of the harder particles. To achieve a comprehensive understanding of the wear mechanisms of NiCrFeBSi coatings subjected to different heat treatment regimes, a morphological analysis of the wear track was carried out using scanning elec-

tron microscopy (SEM), as illustrated in Figure 9. This approach was chosen due to the nature of the tribological data obtained and the need for visual confirmation of the proposed processes.

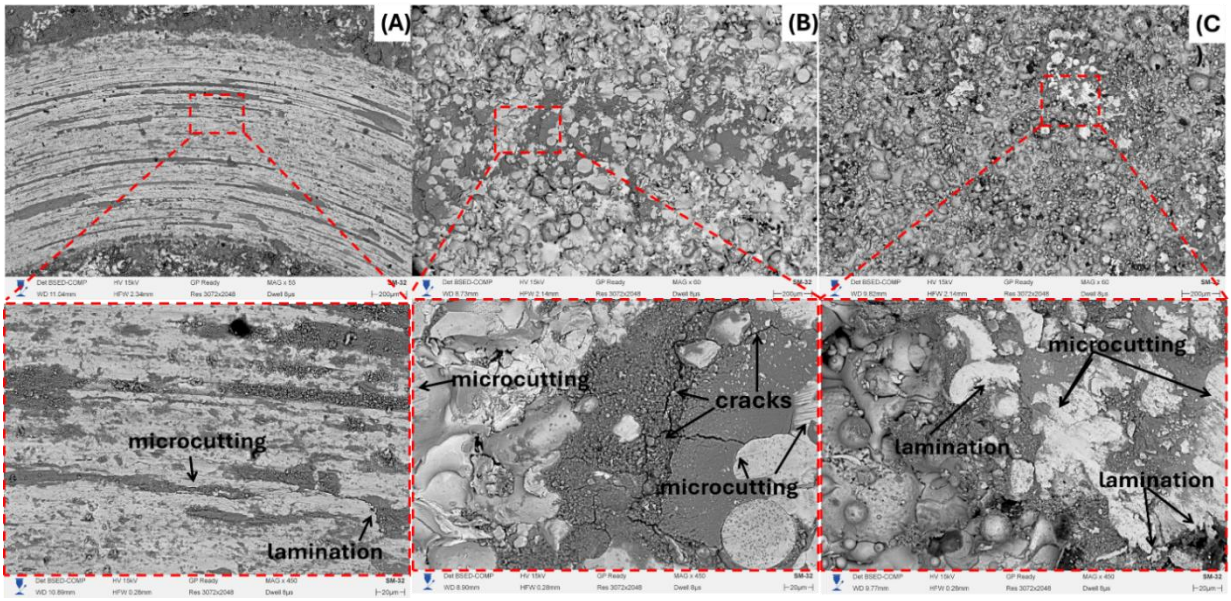

Figure 9. Results of tribological tests using the ball-on-disk scheme under dry friction.
(*A*) without heat treatment SF1, (*B*) after gas-flame heating SF2, (*C*) after heating in a furnace SF3

On the surface of the coating after flame heating, distinct micro-grooves formed during friction, as well as cracks, can be clearly observed. In this context, the micro-grooves result from local abrasive interactions of the counter body with surface inclusions or irregularities of the coating, leading to the removal of microparticles and the formation of elongated traces on the surface. Such areas are often formed in zones where hard phases (carbides, borides) partially protrude above the softer matrix and act as abrasives during sliding. Cracks are formed both along particle boundaries and within the binder phase, indicating a brittle fracture mechanism [29-30].

After furnace treatment, the wear track surface appears more uniform and denser. Although traces of micro-grooves are also present, they are distributed less chaotically and exhibit smaller depth and length. Local layering was also observed, likely occurring along the boundaries of fused particles or between regions with different phase densities. Nevertheless, the overall surface condition confirms a lower degree of wear. This correlates with the low and stable coefficient of friction (0.138 ± 0.003) and indicates a micro-abrasive but plastically adaptive wear mechanism.

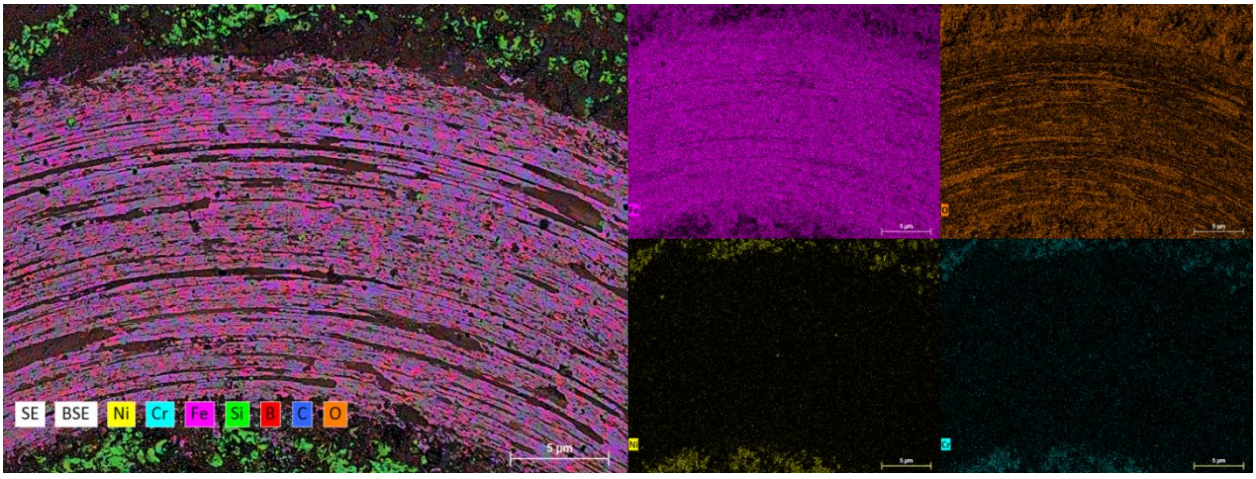

Figure 10. Energy dispersive spectral map (EDS) of the wear track surface of NiCrFeBSi coating after furnace heat treatment

The presented EDS map confirms that the wear track zone represents the product of intense interaction between the coating and the counter body, accompanied by mechanical damage and thermo-oxidative effects (Fig. 10). The main source of iron in the wear track is the counter body (e.g., a ball made of 100Cr6 steel or an equivalent structural steel). During sliding, especially under localized heating, material transfer from the counter body to the coating surface occurs. The iron worn off from the counter body undergoes surface oxidation, resulting in the formation of iron oxides within the wear track.

The formation of such oxide products of friction is characteristic of oxidative wear, in which oxide films develop on the surface. These films may temporarily reduce the coefficient of friction, but upon their breakdown, they become a source of abrasive particles that accelerate wear [31].

The potentiodynamic curves of all coatings show a significantly higher corrosion potential (Ecorr) compared to AISI 1045 steel (Fig. 11).

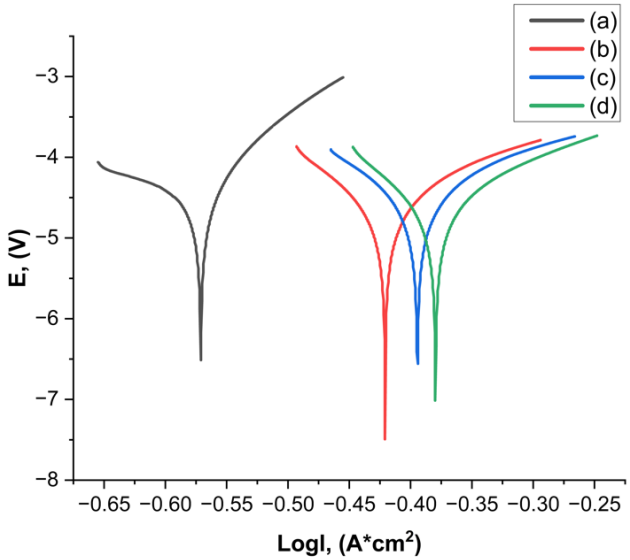

Figure 11. Potentiodynamic curves (*A*) original steel (*B*) without heat treatment SF1, (*C*) after gas flame heating SF2, (*D*) after heating in a furnace SF3

To describe in detail the corrosion behavior of the samples, the corrosion current was calculated from the slopes of the Tafel sections of the potentiodynamic curves (Table 3).

Table 3

Results of measuring the corrosion resistance of self-fluxing NiCrFeBSiC coatings

Samples	Original Steel AISI 1045	SF1	SF2	SF3
Icorr (A)	0.69218	0.42371	0.39466	0.38963
icorr (A/cm^2)	0.881757962	0.539757962	0.502751592	0.496343949
CR (mm/a)	0.0100873122	0.006174832	0.005751479	0.005678175

The data presented in Table 3 and the potentiodynamic polarization curves show a significant difference in the corrosion resistance of the various types of coatings applied to steel. The table includes key parameters such as corrosion current density (Icorr) and corrosion rate (C.R.), which reflect the materials' behavior in corrosion tests. The coating subjected to furnace heat treatment demonstrates the best performance, with an Icorr value of 0.49634 and a corrosion rate of 0.005678, which are considerably lower compared to other coatings, including AISI 1045 steel and coatings treated by flame heating or left untreated. On the potentiodynamic polarization curve, the plot corresponding to AISI 1045 steel shifts into a more negative potential region, confirming its high corrosion activity. This is consistent with the data in the table, where the corrosion current density and corrosion rate for steel are the highest. In contrast, coatings subjected to subsequent flame heating exhibit improved results; however, their corrosion resistance still remains inferior to that of the furnace-treated coating. Such a combination of processing conditions appears to create a denser and more corrosion-protective surface, which prevents the formation of microcracks and moisture retention, thereby

significantly slowing down the corrosion process. Overall, the coatings treated in the furnace showed the best corrosion resistance among all studied variants, making them the most promising for applications requiring protection against aggressive environments.

The data obtained from the adhesion strength measurements characterize the bonding force between the coating and the substrate (base material), which is one of the key quality indicators of thermally sprayed coatings. The results of the adhesion strength tests are presented in the summary of results (Table 4).

Table 4

Summary table of the results of the study of the properties of the characteristics of self-fluxing NiCrFeBSi coatings

Sample name	Adhesion strength, MPa	Microhardness HV_5GPa	Wettability, º	Friction coefficient	Roughness, μm
SF1	18	528.7±2.3	53.152	0.648±0.070	31.860±0.290
SF2	27	771.6±4.6	79.875	0.173±0.050	14.915±0.047
SF3	34	922.4±5.7	89.603	0.138±0.003	13.388±0.016

The results of contact angle measurements performed using the sessile drop method with an optical goniometer are also presented in Table 4. The data indicate a significant influence of the heat treatment regime on the wettability of the coating surfaces. The lowest contact angle (53.152°) was recorded for the coating without additional heat treatment. This suggests high surface energy and a possible microporous structure that promotes oil wetting. After flame heat treatment, the contact angle increased to 79.875°, which can be explained by densification of the structure, partial sintering of particles, and reduction of surface microroughness. The highest contact angle (89.603°) was observed in the furnace-treated sample, which may be associated with the formation of a more uniform, dense, and possibly oxidized layer with reduced wettability. Thus, it can be concluded that heat treatment reduces wettability, which may be a positive factor for the operation of coatings under oil-lubricated friction conditions.

Figure 12 presents SEM images of indenter impressions obtained from microhardness testing of NiCrFeBSiC coatings subjected to different types of heat treatment. Examination of the impressions made it possible to establish correlations between the type of thermal treatment, the microstructural state, and the local hardness of the material. Figure 12(*A*) shows the indenter impression on the coating without heat treatment. Cracks and depressions in the indentation area are clearly visible, associated with the presence of a pore beneath the surface layer. Such local load-bearing instability leads to a reduced microhardness of 528.7 ± 2.3 HV. The data indicate high brittleness of the coating without additional thermal stabilization. Figure 12(*B*) illustrates the structure of the coating after flame heating. In this case, the structure is denser compared to the untreated sample. The impression has a symmetrical shape, and the number of cracks is reduced. The microhardness is 771.6 ± 4.6 HV, which indicates partial structural stabilization and a reduction in internal stresses. Figure 12(*C*) corresponds to the coating subjected to furnace heating. Here, minimal surface damage around the indentation is observed, with no pronounced cracks or depressions, indicating high structural integrity. This is reflected in the highest microhardness value—922.4 ± 5.7 HV—confirming the effectiveness of furnace heat treatment in improving the mechanical properties of the coating.

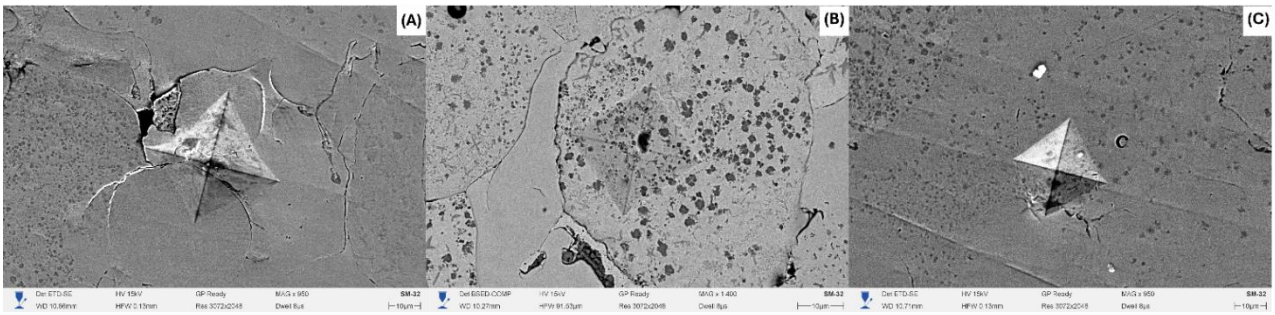

Figure12. SEM images of indenter imprints on NiCrFeBSiC coatings:
(*A*) without heat treatment, (*B*) after flame heating, (*C*) after heating in a furnace

Conclusion

In this study, a comprehensive investigation was carried out on the structural, surface, and tribological characteristics of self-fluxing NiCrFeBSi alloy coatings deposited by flame spraying. It was established that subsequent heat treatment has a significant influence on the formation of the microstructure, phase composition, and performance properties of the coatings. X-ray diffraction analysis revealed the formation of carbide phases (Cr_7C_3, $Cr_{23}C_6$) and intermetallic compounds ($FeNi_3$). Profilometric measurements and SEM micrographs confirmed that uniform furnace heating contributes to a substantial reduction in surface roughness (down to Ra = 13.388 μm), the formation of a dense and homogeneous structure, and the elimination of porosity and defects typical of coatings without additional treatment.

The results of tribological testing showed that the most stable friction characteristics were demonstrated by the coating subjected to furnace heat treatment: the coefficient of friction was 0.138 ± 0.003 and remained constant throughout the entire wear track. In contrast, coatings without heat treatment or treated by flame heating exhibited higher and less stable friction coefficients, accompanied by increased abrasive wear and the formation of microcracks. Elemental analysis of the wear track revealed the presence of wear products in the form of iron oxides originating from the counter body, confirming the contribution of oxidative and adhesive components to the wear mechanism. Thermal treatment—particularly furnace heating—was found to improve the microhardness of the coating by reducing porosity, stabilizing the binder, and enhancing phase distribution. Thus, uniform furnace heat treatment under an optimal temperature regime significantly enhances the service properties of NiCrFeBSi coatings and can be recommended for improving the reliability and durability of protective layers under dry sliding conditions.

Acknowledgment

This research is funded by the Science Committee of the Ministry of Science and Higher Education of the Republic of Kazakhstan (Grant No. BR24992876).

References

1 Kusumar, Nerlfi. Growney. Third global paint & coatings report, 2016–2021, (n.d.). https://www.coatingsworld.com/issues/2017-09-01/view_market-research/kusumgar-nerlfi-amp-growney-publish-third-global-p/ (accessed May 13, 2025).

2 Pawlowski, L. (2008). *The Science and Engineering of Thermal Spray Coatings*. 2nd ed. John Wiley & Sons, Ltd, UK.

3 Havrlisan, S., Simunovic, K., & Vukelic, D. (2006). Modelling of abrasive wear of Ni-based self- fluxing alloy coatings by the application of experimental design. *Technical Gazette, 23*(6), 1687–1693. https://doi.org/10.17559/TV-20161020210442.

4 García, A., Fern´andez, M.R., Cuetos, J.M., Gonz´alez, R., Ortiz, A., & Cadenas, M. (n.d.). Study of the sliding wear and friction behavior of WC + NiCrBSi laser cladding coatings as a function of actual concentration of WC reinforcement particles in ball-on-disk test. *Tribol. Lett*., *63*, 41. https://doi.org/10.1007/s11249-016-0734-3.

5 Guo, C., Zhou, J., Chen, J., Zhao, J., Yu, Y., & Zhou, H. (2011). High temperature wear resistance of laser cladding NiCrBSi and NiCrBSi/WC-Ni composite coatings. *Wear*, *270*, 492–498. https://doi.org/10.1016/j.wear.2011.01.003.

6 Górka, J., Lont, A., & Poloczek, T. (2025). The Microstructure and Properties of Laser Cladded Ni Based Self Fluxing Alloy Coatings Reinforced by TiC Particles. *Coatings*, *15*(5), 527. https://doi.org/10.3390/coatings15050527.

7 Wang, Y., Stella, J., Darut, G., Poirier, T., Liao, H., & Planche, M.-P. (2017). APS prepared NiCrBSi-YSZ composite coatings for protection against cavitation erosion. *J. Alloys Compd*., *699*, 1095–1103. https://doi.org/10.1016/j.jallcom.2017.01.034.

8 Buitkenov, D., Rakhadilov, B., Nabioldina, A., Mukazhanov, Y., Adilkanova, M., & Raisov, N. (2024). Investigation of Structural Phase, Mechanical, and Tribological Characteristics of Layer Gradient Heat-Protective Coatings Obtained by the Detonation Spraying Method. *Materials*, *17*(21), 5253. https://doi.org/10.3390/ma17215253.

9 Sagdoldina, Z., Baizhan, D., Sulyubayeva, L., Berdimuratov, N., Buitkenov, D., & Bolatov, S. (2024). Effect of Electrofriction Treatment on Microstructure, Corrosion Resistance and Wear Resistance of Cladding Coatings. *Coatings*, *14*, 1433. https://doi.org/10.3390/coatings14111433.

10 Xiao, J.-K., Wu, Y.-Q., Zhang, W., Chen, J., Wei, X.-L., & Zhang, C. (2019). Microstructure, wear and corrosion behaviors of plasma sprayed NiCrBSi-Zr coating. *Surf. Coat. Technol*., *360*, 172–180. https://doi.org/10.1016/j.surfcoat.2018.12.114.

11 Rakhadilov, B., Satbayeva, Z., Ramankulov Sh., Shektibayev N., Zhurerova L., Popova N., Uazyrkhanova G., & Sagdoldina, Z. (2021). Change of 0.34Cr-1Ni-Mo-Fe Steel Dislocation Structure in Plasma Electrolyte Hardening. Change of 0.34Cr-1Ni-Mo-Fe Steel Dislocation Structure in Plasma Electrolyte Hardening. *Materials*, *14*(8), DOI: 10.3390/ma14081928

12 Chen, T., Wu, F., Wang, H., & Liu, D. (2018). Laser cladding in-situ Ti(C, N) particles reinforced Ni-based composite coatings modified with CeO_2 nanoparticles. *Metals*, 8. https://doi.org/10.3390/met8080601.

13 Rakhadilov, B., Buitkenov, D., Sagdoldina, Z., Idrisheva, Z., Zhamanbayeva, M., & Kakimzhanov, D. (2021). Preparation and Characterization of NiCr/NiCr-Al_2O_3/Al_2O_3 Multilayer Gradient Coatings by Gas Detonation Spraying. *Coatings*, *11*, 1524. https://doi.org/10.3390/coatings11121524.

14 Houdková, Š., Smazalová, E., Vostřák, M., & Schubert, J. (2014). Properties of NiCrBSi coating, as sprayed and remelted by different technologies. *Surface and Coatings Technology*, *253*, 14–26. doi:10.1016/j.surfcoat.2014.05.009

15 Rakhadilov, B., Pogrebnjak, A., Sagdoldina, Zh., Buitkenov, D., Beresnev, V., & Mukhamedova, A. (2022). Effect of Bilayer Thickness and Bias Potential on the Structure and Properties of (TiZr/Nb)N Multilayer Coatings as a Result of Arc-PVD Deposition. *Materials*, *15*, 7696. https://doi.org/10.3390/ma15217696

16 Kazamer, N., Vălean, P., Pascal, D.-T., Muntean, R., Mărginean, G., & Şerban, V.-A. (2021). Development, optimization, and characterization of NiCrBSi-TiB_2 flame-sprayed vacuum fused coatings. *Surface and Coatings Technology*, *406*, 126747. doi:10.1016/j.surfcoat.2020.126747

17 Rakhadilov, B., Sulyubayeva, L., Maulet, M., Sagdoldina, Z., Buitkenov, D., & Issova, A. (2024). Investigation of High-Temperature Oxidation of Homogeneous and Gradient Ni-Cr-Al Coatings Obtained by Detonation Spraying. *Coatings*, *14*, 11. https://doi.org/10.3390/coatings14010011.

18 Dzhurinskiy, D., Babu, A., Pathak, P., Elkin, A., Dautov, S., & Shornikov, P. (2021). Microstructure and wear properties of atmospheric plasma-sprayed Cr_3C_2-NiCr composite coatings. *Surface and Coatings Technology*, *428*, 127904, ISSN 0257-8972. https://doi.org/10.1016/j.surfcoat.2021.127904.

19 Meiirbekov, M., Ismailov, M., Kenzhegulov, A., Mustafa, L., & Tashmukhanbetova, I. (2024). Study of the effect of combined reinforcement and modification of epoxy resin with rubbers on the impact strength of carbon fiber-reinforced plastic. *Eurasian Journal of Physics and Functional Materials*, *8*(1), 3. https://doi.org/10.32523/ejpfm.2024080103

20 Rojacz, H., Zikin, A., Mozelt, C., Winkelmann, H., & Badisch, E. (2013). High temperature corrosion studies of cermet particle reinforced NiCrBSi hardfacings. *Surf. Coat. Technol.*, *222*, 90–96.

21 Bakhytuly N., Kenzhegulov A.K., Nurtanto M., Aliev A.E., & Kuldeev E.L. (2023). Microstructure and tribological study of TiAlCN and TiTaCN coatings. *Complex Use of Mineral Resources*, *327*(4), 99–110. https://doi.org/10.31643/2023/6445.45.

22 Miguel, J.M., Guilemany, J.M., & Vizcaino, S. (2003). Tribological study of NiCrBSi coating obtained by different processes. *Tribol. Int.*, *36*, 181–187. http://dx.doi.org/10.1016/S0301-679X(02)00144-5.

23 González, R., García, M.A., Peñuelas, I., Cadenas, M., Fernández, M.D.R., & Battez, A. H. (2007). Microstructural study of NiCrBSi coatings obtained by differ ent processes. *Wear*, *263*, 619–624. http://dx.doi.org/10.1016/j.wear.2007.01.094.

24 Fernández, E., Cadenas, M., González, R., Navas, C., Fernández, R., & De Dambor enea J. (2005). Wear behaviour of laser clad NiCrBSi coating. *Wear*, *259*, 870–875. http://dx.doi.org/10.1016/j.wear.2005.02.063.

25 Hemmati, I. (2011). Evolution of microstructure and properties in laser cladding of a Ni–Cr–B–Si hardfacing alloy. *Surf. Eff. Contact Mech*. http://dx.doi.org/10.2495/SECM110.

26 Hemmati, I., Ocelík, V., & De Hosson, J.T.M. (2012). Dilution effects in laser cladding of Ni Cr–B–Si–C hardfacing alloys. *Mater. Lett.*, *84*, 69–72.

27 Reinaldo, P.R. & D'Oliveira, A.S.C.M. (2012). NiCrSiB coatings deposited by plasma transferred arc on different steel substrates. *J. Mater. Eng. Perform.*, *22*, 590–597.

28 Fernandes, F., Cavaleiro, A., & Loureiro, A. (2012). Oxidation behavior of Ni-based coatings deposited by PTA on gray cast iron. *Surf. Coat. Technol.*, *207*, 196–203. https://doi.org/10.1016/j.surfcoat.2012.06.070.

29 Kakimzhanov, D., Rakhadilov, B., Sulyubayeva, L., & Dautbekov, M. (2023) Influence of Pulse-Plasma Treatment Distance on Structure and Properties of Cr_3C_2-NiCr-Based Detonation Coatings. *Coatings*, *13*, 1824. https://doi.org/10.3390/coatings13111824.

30 Riabinkina, P.A., Bataev, I.A., Batraev, I.S., Ruktuev, A.A., Ulianitsky, V.Y., Tanaka, S., Emurlaeva, Y.Y., Ogneva, T.S., & Bataev, V.A. (2022). An Experimental and Numerical Simulation Study of Single Particle Impact during Detonation Spraying. *Metals*, *12*, 1013. https://doi.org/10.3390/met12061013.

31 Rakhadilov, B., Kakimzhanov, D., Baizhan, D., Muslimanova, G., Pazylbek, S., & Zhurerova, L. (2021). Comparative Study of Structures and Properties of Detonation Coatings with α-Al_2O_3 and γ-Al_2O_3 Main Phases. *Coatings*, *11*, 1566. https://doi.org/10.3390/coatings11121566.

Д.Б. Буйткенов, Н.С. Райсов, Н.Е. Базаров, Г.Т. Тлеубергенова,
А.К. Хасенов, Д.Ж. Карабекова

Газды-жалынды бүрку әдісімен алынған өздігінен ағатын никель жабындарының трибологиялық қасиеттерін зерттеу

Жұмыста газды-жалынды бүрку әдісімен жағылған, өздігінен ағатын NiCrFeBSiC қорытпасы негізіндегі жабындардың микроқұрылымы, фазалық құрамы, беткі морфологиясы және трибологиялық сипаттамалары кешенді түрде зерттелді. Әртүрлі жылулық өңдеу түрлерінің — газды-жалынды қыздыру және пеште қыздыру — жабын қасиеттерінің әсеріне ерекше назар аударылды. Рентгендік дифракциялық талдау $FeNi_3$ фазасының, сондай-ақ Cr_7C_3, $Cr_{23}C_6$ карбидтік қосылыстары

мен боридтердің түзілуін анықтады, бұл олардың тозуға төзімділігіне айтарлықтай әсер ететінін көрсетті. Гониометрия әдісімен жүргізілген өлшеулер пеште жылулық өңдеуден өткен жабынның ең жоғары гидрофобтылық қасиетке ие екені айқындалды (жанасу бұрышы — 89,6°). Беткі морфология мен кедір-бұдырлық параметрлері сканерлейтін электронды микроскопия және профилометрия әдістерімен бағаланды, нәтижесінде пештік өңдеу ең тығыз әрі тегіс құрылымды, ең төменгі кедір-бұдырлықпен (Ra = 13,388 мкм) қамтамасыз ететіні анықталды. Өткізілген трибологиялық сынақтар пеште қыздырудан кейінгі жабынның ең төмен және ең тұрақты үйкеліс коэффициентін (0,138 ± 0,003) көрсететінін, бұл тозу изінің микроқұрылымдық ерекшеліктерімен сәйкес келетінін дәлелдеді. Алынған нәтижелер NiCrFeBSiC негізіндегі жабындардың пайдалану қасиеттерін арттыру үшін пештік жылулық өңдеудің жоғары тиімділігін айғақтайды.

Кілт сөздер: өздігінен ағатын қорытпалар, газды-жалынды бүрку, никель қорытпалары, NiCrFeBSi, жылулық өңдеу, 45 болат

Д.Б. Буйткенов, Н.С. Райсов, Н.Е. Базаров, Г.Т. Тлеубергенова,
А.К. Хасенов, Д.Ж. Карабекова

Трибологическое поведение самофлюсующихся покрытий на основе никеля, сформированных газопламенным напылением

В данной работе проведено комплексное исследование микроструктуры, фазового состава, поверхностной морфологии и трибологических характеристик покрытий на основе самофлюсующегося сплава NiCrFeBSiC, нанесённых методом газопламенного напыления. Особое внимание уделено влиянию различных видов термической обработки — газопламенного нагрева и нагрева в печи — на свойства покрытий. Рентгенодифракционный анализ выявил образование фазы $FeNi_3$, а также карбидных соединений Cr_7C_3, $Cr_{23}C_6$ и боридов, что оказывает значительное влияние на износостойкость. Методом гониометрии показано, что наибольшую гидрофобность поверхности обеспечивает покрытие, подвергнутое термической обработке в печи (контактный угол — 89.6°). Поверхностная морфология и параметры шероховатости оценены с помощью сканирующей электронной микроскопии и профилометрии, где установлено, что печная обработка обеспечивает наиболее плотную и сглаженную структуру с наименьшей шероховатостью Ra = 13.388 мкм. Проведённые трибологические испытания показали, что покрытие после нагрева в печи демонстрирует наименьший и наиболее стабильный коэффициент трения (0.138 ± 0.003), что коррелирует с микроструктурными особенностями трека износа. Полученные результаты свидетельствуют о высокой эффективности термической обработки в печи для повышения эксплуатационных свойств покрытий на основе NiCrFeBSiC.

Ключевые слова: самофлюсующиеся сплавы, газопламенное напыление, никелевые сплавы, NiCrFeBSi, термическая обработка, сталь 45

Information about the authors

Buitkenov, Dastan — PhD, Leading Researcher, Scientific Research Center “Surface Engineering and Tribology”, S. Amanzholov East Kazakhstan University, Ust-Kamenogorsk, Kazakhstan; e-mail: buitkenov@gmail.com; ORCID ID: https://orcid.org/0000-0002-0239-5849

Raisov, Nurmahanbet (*corresponding author*) — Junior Researcher, Scientific Research Center “Surface Engineering and Tribology”, S. Amanzholov East Kazakhstan University, Ust-Kamenogorsk, Kazakhstan; e-mail: 2002raisov@gmail.com; ORCID ID: https://orcid.org/0009-0007-1698-957X

Bazarov, Nuraly — Researcher, LLP “PlasmaScience”, Ust-Kamenogorsk, Kazakhstan; e-mail: bazarov.nuraly@gmail.com, ORCID ID: https://orcid.org/0009-0001-9182-7016

Tleubergenova, Gulim — Engineer, Scientific Research Center “Surface Engineering and Tribology”, S. Amanzholov East Kazakhstan University, Ust-Kamenogorsk, Kazakhstan; e-mail: gulh7748@gmail.com, ORCID ID: https://orcid.org/0009-0009-4064-5368

Khassenov, Ayanbergen — PhD, Professor, Buketov Karaganda National Research University, Karaganda, Kazakhstan; e-mail:ayanbergen@mail.ru; ORCID ID: https://orcid.org/0000-0002-5220-9469

Karabekova, Dana — PhD, Professor, Buketov Karaganda National Research University, Karaganda, Kazakhstan; e-mail: karabekova71@mail.ru; ORCID ID: https://orcid.org/0000-0001-8776-4414